FIRE AND MATERIALS
Fire Mater. 2010; **34**:55–75
Published online 22 June 2009 in Wiley InterScience (www.interscience.wiley.com). DOI: 10.1002/fam.1009

Calculation of thermal conductivity of gypsum plasterboards at ambient and elevated temperature

A. C. J. de Korte*, † and H. J. H. Brouwers

Department of Civil Engineering, University of Twente, P.O. Box 217, 7500 AE, Enschede, The Netherlands

SUMMARY

Plasterboard often protects steel structures of buildings because it conducts heat slowly and absorbs the heat of the fire by its volumetric enthalpy. The most important property governing the heat transfer is the thermal diffusion. This property depends on the density, specific heat and thermal conductivity. The first two can be calculated based on the mass composition of the board. The thermal conductivity is more difficult to derive since it is a directional property. This paper will focus on the calculation of the thermal conductivity at ambient and elevated temperatures.

It is shown that the thermal conductivity of gypsum plasterboard (i.e. a porous medium) can be assumed to be a three-phase system. Plasterboard consists of a solid phase and a water/air mix in the voids. The differences between different theoretical equations for both dry and moistured plasterboards are presented. The equation proposed by Zehner and Schlunder (*Chem. Ing.-Tech.* 1972; **44**(23):1303–1308) with shape-factor C of 5 gave good agreement with experimental data of the different boards. Furthermore, the influence of the composition of the boards on the thermal conductivity is investigated. This has an influence, especially since the composition is also related to its moisture content. Regression analysis

*Correspondence to: A. C. J. de Korte, Department of Civil Engineering, University of Twente, P.O. Box 217, 7500 AE, Enschede, The Netherlands.
†E-mail: a.c.j.dekorte@ctw.utwente.nl

Contract/grant sponsor: European Commission; contract/grant number: 026661-2
Contract/grant sponsor: Bouwdienst Rijkswaterstaat
Contract/grant sponsor: Rokramix
Contract/grant sponsor: Betoncentrale Twenthe
Contract/grant sponsor: Betonmortelcentrale Flevoland
Contract/grant sponsor: Graniet-Import Benelux
Contract/grant sponsor: Kijlstra Beton
Contract/grant sponsor: Struyk Verwo Groep
Contract/grant sponsor: Hülskens
Contract/grant sponsor: Insulinde
Contract/grant sponsor: Dusseldorp Groep
Contract/grant sponsor: Eerland Recycling
Contract/grant sponsor: Enci
Contract/grant sponsor: Provincie Overijssel
Contract/grant sponsor: Rijkswaterstaat Directie Zeeland
Contract/grant sponsor: A&G Maasvlakte
Contract/grant sponsor: BTE
Contract/grant sponsor: Alvon Bouwsystemen
Contract/grant sponsor: V.d Bosch Beton

points out that the moisture content depends only on the gypsum content. A value of 2.8% absorbed water on the mass of gypsum is found, and this water plays an important role in the thermal conductivity of plasterboard at ambient temperature.

Finally, the thermal conductivity of board at elevated temperature is computed. A close fit between computed and experimental values derived from literature is found.

Received 16 January 2009; Revised 2 April 2009; Accepted 21 April 2009

KEY WORDS: thermal conductivity; gypsum plasterboard; moisture; porous medium

1. INTRODUCTION

The exposure of a structural material, such as steel, to high temperature reduces its strength and rigidity and may lead to structural collapse, when the critical temperature is reached [1]. Two methods are commonly used to protect the steel, namely the insulation and capacitive method [2]. The insulation method consists of attaching insulating material to the external surface of the structure. One of the possible insulation materials is gypsum plasterboard. The capacitive method is based on the principle of using the heat capacity of a protective material to absorb heat. Gypsum uses mainly the insulation method because it conducts heat slowly, but it will also absorb some of the heat of the fire by its volumetric enthalpy. Gypsum plasterboards therefore increase the time until the structural members reach the critical temperature. The most important property governing the heat transfer is the thermal diffusion. The thermal diffusivity provided here can serve as an input for the energy transport models that are used in moisture transfer models [1, 3–5] and fire simulation models [3, 6–10]. The presented work is a part of European project I-SSB, which develops a fire model on three levels (micro, meso and macro level). The output of the presented microstructural work is used in models on meso and macro level. The diffusivity depends on the density, specific heat and thermal conductivity. The first two can be calculated based on the mass composition of the board. The thermal conductivity is more difficult to calculate since it is a directional property. This paper will focus on the considering of local microstructure system rather than the overall moisture and heat transfer model.

The thermal conductivity of materials is more complicated for porous media, which consists of different phases. Kaviany [11] points out that the heat conduction through fully saturated matrix depends on the structure of the matrix and the thermal conductivity of each phase. The same principle applies for any heterogeneous material. One of the most difficult aspects of the analysis of heat conduction through a porous medium is the structural modelling. This is because the representative elementary volumes are three dimensional and have complicated structures that vary greatly among different porous media. Since the thermal conductivity of the solid phase is generally larger than that of the fluid, the manner in which the solid is interconnected influences the conduction.

Furthermore, a plasterboard consists of a solid phase and water/air mix in the voids. The thermal conductivity of the voids depends strongly on the amount of moisture (absorbed water) in the voids, since the thermal conductivity of water is 23 times the thermal conductivity of air. Within this paper a gypsum plasterboard is assumed to be a three-phase system. The calculation of the thermal conductivity of this system is divided into a number of steps. The first step is

DOI: 10.1002/fam

the calculation of the thermal conductivity of two different two-phase porous systems. The first system consists of the solid material and air as the pore fluid, whereas the second system consists of the solid material and liquid water as the pore fluid. Based on the thermal conductivities of these two systems, the thermal conductivity of the porous medium with moistened air as the void fluid can be computed. This concept is applied to various types of gypsum/limestone plasterboards. The models are validated by comparing the results of the models with experiments. Based on these results and models, conclusions are drawn in regard to the amount of absorbed water.

Finally, the concept of thermal conductivity is applied on gypsum plasterboards under fire. When gypsum plasterboard is exposed to fire, the density/void fraction, the structure, the moisture content and the composition of the board will change due to decomposition reactions in the core of the board. These properties influence the thermal conductivity of the boards. The thermal conductivity of the individual solid phases also varies with temperature. The variation of thermal conductivity over certain temperature ranges can be neglected for some materials, but may be significant for others. The thermal conductivity temperature dependence of the considered solids is however limited [12]. Therefore in this research the thermal conductivity of the solid phases is assumed to be the constant, but the thermal conductivity of the composite material (e.g. the gypsum plasterboard) will change due to the changes in the void fraction and composition of the material. The experimental results of plasterboards are compared with the results from simulations derived from the developed model. Based on these results, conclusions are drawn with regard to the applicability of the proposed thermal conductivity model during fire.

2. TWO-PHASE SYSTEMS

For two-phase systems, several equations have been suggested during the last two centuries. Côte and Konrad [13] point out that heat conduction through a two-phase porous media depends on the thermal conductivity as well as the structure of the solid matrix. In terms of thermal behaviour, the structure of the solid matrix determines the contact resistance and the continuity of the solid phase [11]. Hamilton and Crosser [14] showed theoretically that the thermal conductivity of particle packings decreases with increasing sphericity of particles. This effect was also noticed by Johansen [15] and Côté and Konrad [16] in air-saturated geomaterials where the thermal conductivity of natural particle packing (rounded/sub-rounded particles) was systematically lower than those of crushed particle packings (angular/sub-angular particles). A possible reason for this effect could be found in the smaller contact areas among the spherical particles compared with the more angular particles. Since the amount of contact area is related to the possible amount of solid–solid conductivity, which is always more than solid–fluid conductivity.

The most simple calculation methods for the conduction of two-phase media are the serie and parallel conduction. Both methods assume a very simple structure. Porous materials are in fact a large combination of parallel and serie conductivities. Since these thermal networks are complicated, there has been a search for more general equations/methods to describe the thermal conductivity of porous media. The Maxwell equations can be used for this. There are two limits distinguished: the so-called upper and lower bound [17]. The lower bound describes the dilute suspension of particles. The upper bound is a solid body containing dilute inclusion of fluid. Both limits neglect the exact particle shapes within the microstructure.

DOI: 10.1002/fam

There are also methods that take into account both the thermal conductivity of the different phases as well as the specific particle shape. For example Miller [18] introduced a more complicated equation for the upper and lower bound, including a correction for cell shape (G).

The thermal conductivity will be between the upper and lower bound, since the porous material is neither a dilute fluid nor a dilute solid. Hadley [19] introduced therefore the 'weighted average Maxwell equation'. This equation combines an expression describing the conduction through a continuous solid (the upper Maxwell formula) with one describing a suspension of particles. The part for the suspension of particle approaches the lower Maxwell formula when the limit of void fraction tends to unity. This is a valid assumption when assuming that solid spheres are to far apart to interact under the lower Maxwell equation. This weighted average Maxwell equation reads:

$$\lambda_e = \lambda_f \left((1-\alpha_0) \frac{f_0\varphi + \kappa(1-f_0\varphi)}{1-\varphi(1-f_0)+\kappa\varphi(1-f_0)} + \alpha_0 \frac{2\kappa^2(1-\varphi)+(1+2\varphi)\kappa}{(2+\varphi)\kappa+1-\varphi} \right) \tag{1}$$

with

$$\kappa = \lambda_s/\lambda_f \tag{2}$$

λ_e is the effective thermal conductivity of porous medium, λ_f is the thermal conductivity of the pore fluid, λ_s is the thermal conductivity of the solid phase and φ is the void fraction of the porous medium. Equation (1) depends on the value of the mixture factor f_0 and degree of consolidation α_0. The degree of consolidation reads

$$\begin{aligned} {}^{10}\log(\alpha_0) &= -4.898\varphi \quad \text{for } 0 \leqslant \varphi < 0.0827 \\ {}^{10}\log(\alpha_0) &= -0.405 - 3.154(\varphi - 0.0827) \quad \text{for } 0.0827 \leqslant \varphi < 0.298 \\ {}^{10}\log(\alpha_0) &= -1.084 - 6.778(\varphi - 0.298) \quad \text{for } 0.298 \leqslant \varphi \leqslant 0.580 \end{aligned} \tag{3}$$

Figure 1 shows the values of α_0 versus φ based on this equation. From Figure 1 it follows that the degree of consolidation tends to zero when the void fraction tends to unity. Since gypsum plasterboards have normally a void fraction bigger than 0.6, α_0 is zero. Therefore, Equation (1) can be represented by

$$\lambda_e = \lambda_f \left(\frac{f_0\varphi + \kappa(1-f_0\varphi)}{1-\varphi(1-f_0)+\kappa\varphi(1-f_0)} \right) \tag{4}$$

with f_0 as the mixture factor. When the mixture factor is equal to $\frac{2}{3}$, it corresponds to the lower Maxwell equation. When mixture factor is equal to $2\kappa/(2\kappa+1)$, Equation (4) is equal to the upper Maxwell limit. Therefore, the value of f_0 should be between $\frac{2}{3}$ and $2\kappa/(2\kappa+1)$. Hadley [19] points out that the value of f_0 is increasing with $(1-\varphi)$ starting at $\frac{2}{3}$. Unfortunately, there is no proper functional form yet. Hadley [19] introduced a linear function for f_0 of the void fraction, reading;

$$f_0 = 0.8 + 0.1\varphi \tag{5}$$

This linear function does not fit with the upper and lower limit for f_0, which were set by Hadley [19]. Therefore, here a linear function is proposed that is located between the upper and lower limit for f_0;

$$f_0 = \frac{2}{3} + \varphi\left(\frac{2\kappa}{2\kappa+1} - \frac{2}{3} \right) \tag{6}$$

DOI: 10.1002/fam

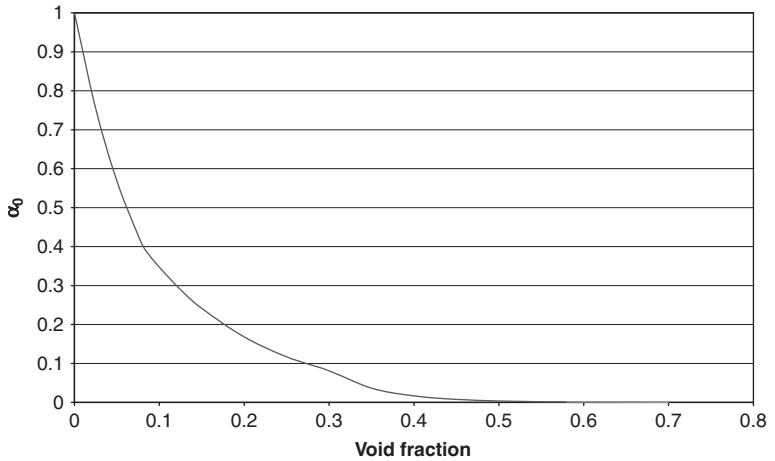

Figure 1. Degree of consolidation (α_0) (Equation (3)) used for the weighted average Maxwell equation versus void fraction.

Table I. The sphericity (ψ) of different particle shapes used to describe the interconnection of particles for the thermal conductivity [14].

Particle shape	Shape factor (ψ)
Sphere	1.0
5:1 cylinder	0.68
10:1 Cylinder	0.57
Parallel pipes	0.62

Another equation for f_0 was proposed by Verma *et al.* [20]

$$\ln f_0 = -\left(\frac{\psi^3}{\kappa}\right)^{1/3} \tag{7}$$

In which ψ is the sphericity of the particles in the matrix. The sphericity of a sphere equals unity and is smaller than unity for non-spherical shapes. Hamilton and Crosser [14] gave the sphericity of different particle shapes. Table I shows the sphericity of the different particle shapes. The sphericity is determined based on the actual surface area of the particle (s) and surface of sphere (S_{sph}) with same volume as the particle and is defined as:

$$\psi = \frac{S_{\text{sph}}}{s} \tag{8}$$

The microstructure of the core of plasterboard is characterized by a needle-like structure. The needle-like structure could be modelled as long cylinders. According to Hamilton and Crosser [14] (Table I), a sphericity of 0.555 corresponds with a long cylinder shape. For $\kappa = 48.3$ (air–gypsum system) Equation (6) yields between $\frac{2}{3}$ and 0.877 for void fraction (φ) of 0.65 and

DOI: 10.1002/fam

Table II. The shape factor (C) for different particle shapes used to describe the interconnection of particles within the thermal conductivity equations [21].

Particle shape	Shape factor (C)
Sphere	1.25
Broken particle	1.40
Cylinder and tubes	2.50
Cementatious material	5.00

Equation (7) equals 0.859 with $\psi = 0.555$. While for $\kappa = 2.09$ (water–gypsum system) Equation (6) yields between 0.667 and 0.758 for $\varphi = 0.65$, and Equation (7) equals 0.648 with $\psi = 0.555$.

Another possibility is to describe the thermal conductivity with the method of Zehner and Schlunder [21]. Zehner and Schlunder, like Miller [18] and Verma [20], take into account the shape of the particles and therefore their surface connectivity. The equation of Zehner and Schlunder reads

$$\lambda_e = \lambda_f(1-\sqrt{1-\varphi}) + \lambda_f\sqrt{1-\varphi}\cdot A \tag{9}$$

with

$$A = \frac{2}{N}\left(\frac{B}{N^2}\frac{\kappa-1}{\kappa}\ln\left(\frac{\kappa}{B}\right) - \frac{B+1}{2} - \frac{B-1}{N}\right)$$

$$N = 1 - \frac{B}{\kappa}$$

$$B = C\left(\frac{1-\varphi}{\varphi}\right)^{10/9}$$

and with κ following from Equation (2). The factor C depends on the form of the particle. The different values for this factor are presented in Table II. These values are for particles that can freely move in/through the matrix. In the case of a gypsum core, there are a high number of so-called solid-phase bridges. This higher connectivity leads to a higher conductivity compared with a system with the same void fraction but with lower connectivity. For such systems with high number of solid-phase bridges, a C-value of 5 is proposed [22].

3. THEORY VERSUS EXPERIMENTAL DATA

This section describes the experimental data on thermal conductivity of gypsum plasterboards found in the literature, which are used to compare with the calculation results obtained by presented equations. This experimental data are often found together with a description of the apparent density and chemical composition. Both these parameters are important in order to predict the thermal conductivity of plasterboards. The density is important because it is closely related to the void fraction of plasterboards. As can be seen in the previous section, the void fraction is one of the main parameters for the calculation of the thermal conductivity. The chemical composition of gypsum plasterboards influences the thermal conductivity of the solid phase within the board.

DOI: 10.1002/fam

Table III. Experimental values of apparent density, chemical composition and thermal conductivity of gypsum plasterboards at room temperature as described in literature.

Source	Apparent density (kg/m^3)	Composition $\%m_{C\bar{S}H_2}$ (kg/kg)	$\%m_{C\bar{C}}$ (kg/kg)	$\%m_{M\bar{C}}$ (kg/kg)	λ_{meas} (W/(m K))
Wullschlager and Ghazi Wakili [23]	810	81	9.5		0.28
Ang and Wang [24]	836				
Mehaffey *et al.* [25] 1	732				0.25
Mehaffey *et al.* [25] 2	648				0.24
Sultan [26]	698				0.25
Ghazi Wakili and Hugi [27] 1	735	80.9	12.3		0.28
Ghazi Wakili and Hugi [27] 2	840	62.2	32.3		0.30
Ghazi Wakili and Hugi [27] 3	740	76.5	4.2	4.7	0.23
Ghazi Wakili and Hugi [27] 4	870	98			0.32

Table III shows values that are presented in literature. It should be noted that most articles on the thermal properties of gypsum plasterboard tend to use the data of Mehaffey *et al.* [25] or Sultan [26]. Ghazi Wakili and Hugi [27] and Wullschlager and Ghazi Wakili [23] performed additional experiments and also determined the chemical composition of the gypsum plasterboard based on the thermal decomposition peaks. The presence of calcium carbonate is confirmed by Oates [28], who points out that calcium carbonate is used by the production of Flue Gas Desulfarization Gypsum (FGD-gypsum). For the production of the plasterboards partly FGD-gypsum is used, which explains the presence of calcium carbonate in plasterboards.

The experimental data are compared with the equations of the previous section. For this comparison the thermal conductivity of the solid needs to be known. Since the solid phase of gypsum plasterboards consists of several phases, the thermal conductivity of the solid phases has to be calculated. There are different calculation methods available for thermal conductivity of the composite solid. Clauser and Huenges [29] mentioned the following three equations for this calculation

$$\lambda_s = \sum \delta_i \lambda_i \tag{10}$$

$$\lambda_s = \frac{1}{\sum \frac{\delta_i}{\lambda_i}} \tag{11}$$

$$\lambda_s = \prod \lambda_i^{\delta_i} \tag{12}$$

with λ_i is the thermal conductivity of $_i$th solid phase and volume fraction of $_i$th solid phase. The summation of the volume fractions (δ_i) equals unity. All three methods provide a thermal conductivity of the solid phase based on the average of the available solid phases while taking into account the volume fraction of the phases. Equation (10) is the arithmetic average. This average assumes that the volume fractions are in series. Equation (11) is the harmonic average, which assumes a parallel arrangement of the ingredients. Equation (12) is the geometric mean method, which seems more realistic. The geometric method cannot be linked to a clear defined physical model, as is the case for the arithmetic and harmonic average. The geometric mean is a type of average that indicates the central tendency or typical value of a set of numbers, and is often used

DOI: 10.1002/fam

Table IV. Thermal conductivities and specific density of the used substances.

Substance	Thermal conductivity (W/(m K))	Specific density (kg/m^3)
$CaSO_4 \cdot 2H_2O$	1.255	2310
$CaCO_3$	3.58	2720
$MgCO_3$	5.83	2990
Liquid water	0.60	1000
Air (dry)	0.026	1.3

for exponential data. Côté and Konrad [16] use the third method for their calculation of the thermal conductivity of dry soil.

All three methods are used for the calculation of the thermal conductivity of the complete solid-phase based on the thermal conductivity of the individual phases. All three methods use the volume-based composition. In order to get the volume-based composition from the mass-based composition, the specific densities of the different solid phases need to be known. The thermal conductivities and specific densities of the individual substances used are presented in Table IV. Figure 2 shows the effects on the solid thermal conductivity, when replacing gypsum by calcium carbonate. Table V shows the results of the thermal conductivity of the solid phase of plasterboards based on Equations (10)–(12), the chemical composition from Table III and properties from Table IV. It can be noticed from Table V that the three equations for the calculation of the thermal conductivity of the solid based on the chemical composition of the solid phase result in large differences. The difference can be up to 33% between the arithmetic and harmonic method. In general the harmonic method will deliver the lowest value, while the highest value is obtained with the arithmetic method. The geometric method leads to a value in between. Since the microstructure of porous medium is also in between the serie and parallel arrangement and usually a combination of these extreme cases, it seems the most realistic model for the calculation of the solid thermal conductivity. According to Clauser and Huenges [29] both the arithmetic and harmonic methods have the disadvantage of describing the special cases and therefore are given the upper and lower boundaries. They point out that the geometric method is quite successfull in predicting the thermal conductivity in many cases. Furthermore the geometric method was also recommended by Côté and Konrad [16].

Next, the two-phase conductivities are computed based on the expressions from Section 2 and the calculated solid thermal conductivities from Table V. The results of these computations are presented in Table VI and Figure 3. From Table VI and Figure 3 it could be concluded that the measured value is between upper and the lower bound of the Maxwell. The upper Miller limit is in some cases larger than measured value. The weighted average Maxwell, the equation of Hadley and the equation of Zehner and Schlunder are all smaller than the measured value. A good agreement was obtained with weighted average Maxwell, and with Zehner and Schlunder with $C = 5$.

The calculation method for the solid has an influence on the results. The highest thermal conductivity is obtained with the arithmetic and lowest with the harmonic method. The obtained geometric value is in between. These findings are in line with the findings based on only the thermal conductivity of the solid phase.

DOI: 10.1002/fam

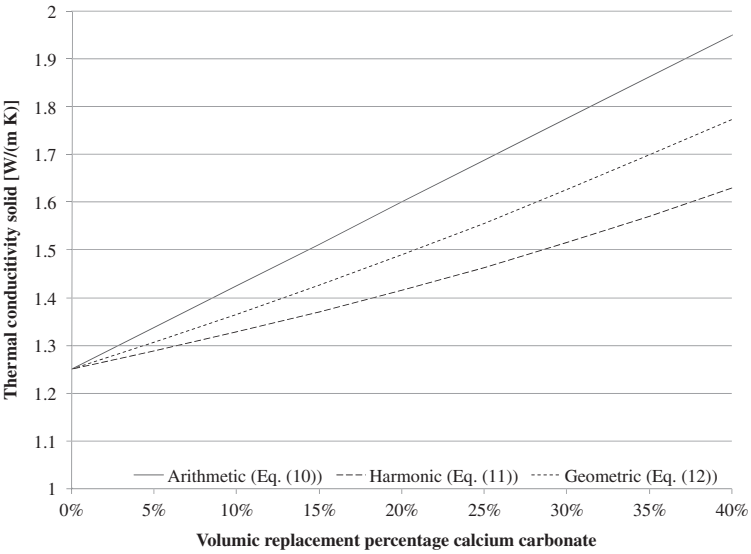

Figure 2. Thermal conductivity of gypsum and calcium carbonate compounds for three mixing/calculation equations (Equation (10)–(12)).

Table V. The results of the calculation of the solid thermal conductivity for the solid phase only based on the three methods mentioned by [29].

	Arithmetic (Equation (10))	Harmonic (Equation (11))	Geometric (Equation (12))
Wullschlager and Ghazi Wakili [23]	1.47	1.33	1.38
Mehaffey *et al.* [25] 1	1.26	1.26	1.26
Mehaffey *et al.* [25] 2	1.26	1.26	1.26
Sultan [26]	1.26	1.26	1.26
Ghazi Wakili and Hugi [27] 1	1.52	1.36	1.42
Ghazi Wakili and Hugi [27] 2	1.97	1.57	1.72
Ghazi Wakili and Hugi [27] 3	1.56	1.34	1.40
Ghazi Wakili and Hugi [27] 4	1.26	1.26	1.26

The obtained value from the equations of both Hadley [19] and Zehner and Schlunder [21] are too low compared with the results obtained from experiments. This could be the result of the current assumption that the voids are filled with dry air, while in reality the fluid in the voids is usually moistured. Building materials, such as gypsum plasterboards, are porous media in which moisture transfer occurs in both the vapor/gas and liquid phase. Bouguerra [30] points out that the thermal conductivity is strongly influenced by the moisture content migrating through porous material. Since the thermal conductivity of water vapour is similar to the thermal conductivity of air, there will be no clear difference. But the thermal conductivity of liquid water is 23 times the thermal conductivity of air which will lead to a clear difference. The next section will focus on the effect of moisture on the thermal conductivity of the gypsum plasterboards.

DOI: 10.1002/fam

Table VI. Results of different theoretical equations from literature for the dry thermal conductivity.

	λ_{meas}	A	B	C	D	E	F	G	H	I	$I2$	J	$J2$
Wullschlager and Ghazi Wakili [23]	0.28	(10)	0.039	0.517	0.398	0.064	0.287	0.076	0.164	0.118	0.110	0.119	0.171
Wullschlager and Ghazi Wakili [23]	0.28	(11)	0.039	0.477	0.368	0.064	0.267	0.075	0.160	0.116	0.107	0.116	0.165
Wullschlager and Ghazi Wakili [23]	0.28	(12)	0.039	0.493	0.381	0.064	0.275	0.075	0.161	0.107	0.108	0.117	0.167
Mehaffey *et al.* [25] 1	0.25		0.038	0.416	0.319	0.059	0.223	0.068	0.144	0.097	0.096	0.103	0.145
Mehaffey *et al.* [25] 2	0.24		0.036	0.371	0.282	0.054	0.186	0.060	0.129	0.092	0.085	0.090	0.126
Sultan [26]	0.25		0.037	0.397	0.304	0.057	0.208	0.065	0.138	0.095	0.092	0.097	0.137
Ghazi Wakili and Hugi [27] 1	0.28	(10)	0.038	0.492	0.375	0.059	0.257	0.068	0.150	0.105	0.100	0.106	0.152
Ghazi Wakili and Hugi [27] 1	0.28	(11)	0.038	0.441	0.337	0.059	0.233	0.067	0.145	0.111	0.097	0.103	0.146
Ghazi Wakili and Hugi [27] 1	0.28	(12)	0.038	0.459	0.351	0.059	0.241	0.067	0.147	0.104	0.098	0.104	0.149
Ghazi Wakili and Hugi [27] 2	0.30	(10)	0.039	0.695	0.533	0.064	0.379	0.077	0.177	0.127	0.121	0.129	0.189
Ghazi Wakili and Hugi [27] 2	0.30	(11)	0.039	0.557	0.429	0.064	0.308	0.076	0.167	0.120	0.113	0.121	0.175
Ghazi Wakili and Hugi [27] 2	0.30	(12)	0.039	0.614	0.471	0.064	0.337	0.076	0.171	0.124	0.117	0.125	0.181
Ghazi Wakili and Hugi [27] 3	0.23	(10)	0.038	0.505	0.385	0.059	0.264	0.068	0.152	0.103	0.102	0.108	0.154
Ghazi Wakili and Hugi [27] 3	0.23	(11)	0.038	0.438	0.335	0.059	0.232	0.068	0.146	0.111	0.097	0.104	0.147
Ghazi Wakili and Hugi [27] 3	0.23	(12)	0.038	0.458	0.350	0.059	0.242	0.068	0.148	0.101	0.099	0.105	0.149
Ghazi Wakili and Hugi [27] 4	0.32		0.041	0.489	0.382	0.069	0.289	0.083	0.172	0.105	0.116	0.128	0.181

A: λ_S calculation method by Equations (10)–(12). B: serie. C: parallel . D: Maxwell upper bound. E: Maxwell lower bound. F: Miller upper bound. G: Miller lower bound. H: weighted average Maxwell. I: Hadley (Equation (4)) with Equation (6) for f_0. I2: Hadley (Equation (4)) with Equation (7) for f_0. J: Zehner and Schlunder (Equation (9)) with $C = 2.5$. J2: Zehner and Schlunder (Equation (9)) with $C = 5.0$.

DOI: 10.1002/fam

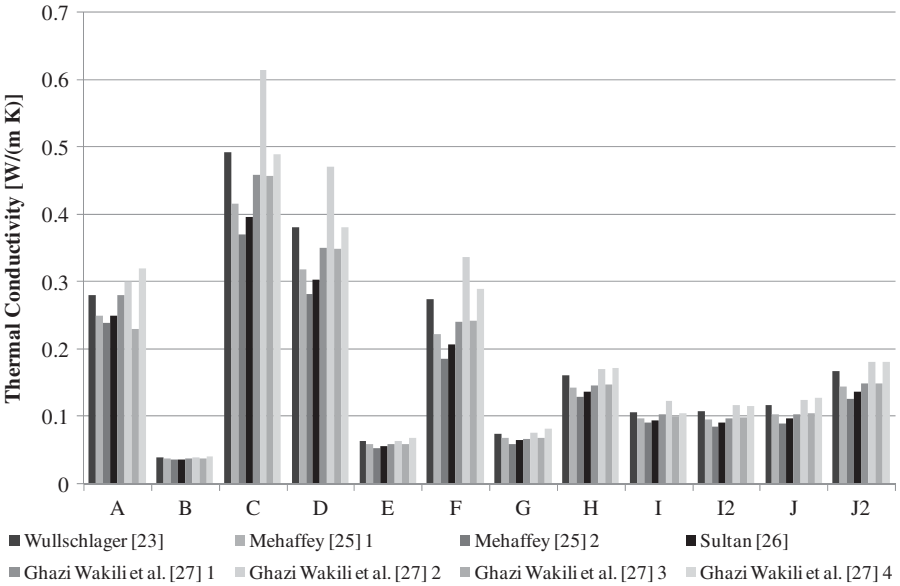

Figure 3. Thermal conductivity at ambient temperature for the different plasterboards with A the measured values and B-J2 the computed values. (A): measured; (B): serie; (C): parallel; (D): Maxwell upper bound; (E): Maxwell lower bound; (F): Miller upper bound; (G): Miller lower bound; (H): weighted average Maxwell; (I): Hadley (Equation (4)) with Equation (6) for f_0; (I2): Hadley (Equation (4)) with Equation (7) for f_0; (J): Zehner and Schlunder (Equation (9)) with $C=2.5$; (J2): Zehner and Schlunder (Equation (9)) with $C=5.0$.

4. THREE-PHASE SYSTEM

The considered three-phase system consists of a solid porous medium with a mixture of a liquid (water) and a gas (dry air) in the voids. Somerton *et al.* [31] have derived the following equation for porous medium filled by a mixture of two fluids:

$$\lambda_e = \lambda_g + \sqrt{s_l}(\lambda_l - \lambda_g) \tag{13}$$

here λ_g is the effective thermal conductivity of the porous medium filled with dry air, λ_f is the effective thermal conductivity of the porous medium filled with water and the volume-based saturation rate of fluid in the voids. Both λ_g and λ_l can be calculated with the equations for two-phase effective conductivity given in Section 2, with λ_{air} and λ_{water} as the λ_f, respectively.

Here, the method proposed by Somerton *et al.* [31] is used to derive the amount of water needed to comply with the thermal conductivity as measured in the literature. During this derivation the effect of the moisture on apparent (wet) density needs to be taken into account. The apparent density consists of the dry density and the effect of moisture on the density. The dry density is related to the void fraction of the material. So the density, void fraction and moisture content are

DOI: 10.1002/fam

all interrelated. This relation reads:

$$\rho_e = \rho_g \cdot (1-\varphi) + \rho_l \cdot \varphi \cdot s_l \tag{14}$$

With ρ_e the wet (apparent) density of the board, ρ_g the dry specific solid density, ρ_l the density of the water, φ the void fraction and s_l the volume-based saturation rate of void fluid.

Table VII and Figure 4 shows the results of the derived moisture content in the voids based on both the Hadley (weighted average Maxwell) and the Zehner and Schlunder equations with the use of the three different equations for the solid-phase thermal conductivity. As shown in Table VII the calculation method for the solid thermal conductivity has an influence on the deduced water amount. The introduced water amount is lowest for the arithmetic (Equation (10)) and is highest for harmonic method (Equation (11)). This is exactly the opposite to the dry thermal conductivity, where the arithmetic method gives the highest thermal conductivity and the harmonic method the lowest conductivity. This seems logical since there is less water introduced to comply with the measured value.

Furthermore, the values derived from the Zehner and Schlunder equation are lower than the values derived with the Hadley and weighted average Maxwell equation. The sorbed water values following from Hadley, Zehner and Schlunder and weighted average Maxwell equation are all in line with values from literature. Ang and Wang [24] also give a moisture content of 3% m/m. This value is furthermore mentioned by Thomas [32], and Belmiloudi and Le Meur [6]. Therefore, one can conclude that all three equations are close to the values from literature, with Zehner and Schlunder being closest.

The results from Table VII can be analysed even further to see if there is any parameter explaining the difference between the moisture contents of the different boards. Based on knowledge of the composition of gypsum boards, one can derive the following hypotheses:

(1) The moisture content depends on the total mass of the solid.
(2) The moisture content depends on the mass of the gypsum.
(3) The moisture content depends on the masses of the gypsum and the limestone.

In order to verify these hypotheses, a regression analysis on the obtained data is performed to find if there is any relation between the solid composition and the absorbed amount of water. This is done for all three equations with the use of the three solid thermal conductivity equations in order to check the dependences of the solid thermal conductivity on the effective thermal conductivity.

Table VIII and Figure 5 show the analysis performed on the results of the three equations and three solid calculation methods. Both hypothesis 1 and 2 gave stable results for all methods, for calcium carbonate no reliable amount of water could be deduced. The best results are obtained for hypothesis 2, because it delivers the smallest average error and smallest maximum error with the smallest number of parameters, i.e. implying that limestone does not contain moisture. Furthermore, in general the best results were obtained with the geometric method for the calculation of the solid thermal conductivity. The difference between the different solid conductivity calculation methods is around 0.3%. Therefore, the influence is limited and all three equations could be used. The regression coefficient for gypsum is in line with the value found in literature for the sorption and desorption of water. Thomas [32], for instance, gives a moisture content of 3% m/m, a value confirmed by Belmiloudi and Le Meur [6].

DOI: 10.1002/fam

Table VII. Water content (m/m) needed to match the measured thermal conductivity for the three different methods with *A* the arithmetic method, *G* the geometric method and *H* the harmonic method.

	Weighted average Maxwell [19]			Zehner and Schlunder [21] $C=5$		
	A (%)	*H* (%)	*G* (%)	*A* (%)	*H* (%)	*G* (%)
Wullschlager and Ghazi Wakili [23]	2.50	3.00	2.81	1.81	2.25	2.08
Mehaffey *et al.* [25] 1	2.85	2.85	2.85	2.32	2.32	2.32
Mehaffey *et al.* [25] 2	3.90	3.90	3.90	3.42	3.42	3.42
Sultan [26]	3.51	3.51	3.51	2.95	2.95	2.95
Ghazi Wakili and Hugi [27] 1	3.75	4.55	4.23	2.93	3.66	3.37
Ghazi Wakili and Hugi [27] 2	1.96	3.02	2.50	2.28	2.16	1.72
Ghazi Wakili and Hugi [27] 3	1.22	1.64	1.49	0.92	1.32	1.78
Ghazi Wakili and Hugi [27] 4	4.45	4.45	4.45	3.24	3.24	3.24
	Hadley [19]			Miller Upper [18]		
	A (%)	*H* (%)	*G* (%)	*A* (%)	*H* (%)	*G* (%)
Wullschlager and Ghazi Wakili [23]	2.47	2.96	2.77		0.02	
Mehaffey *et al.* [25] 1	2.58	2.58	2.57	0.15	0.15	0.15
Mehaffey *et al.* [25] 2	3.20	3.20	3.20	0.86	0.86	0.86
Sultan [26]	3.06	3.06	3.06	0.46	0.46	0.46
Ghazi Wakili and Hugi [27] 1	3.34	4.11	3.81	0.07	0.55	0.32
Ghazi Wakili and Hugi [27] 2	1.93	2.97	2.46			
Ghazi Wakili and Hugi [27] 3	1.01	1.42	1.28			
Ghazi Wakili and Hugi [27] 4	4.69	4.69	4.69	0.21	0.21	0.21

A: Solid thermal conductivity according to arithmetic average (Equation (10)).

H: Solid thermal conductivity according to harmonic average (Equation (11)).

G: Solid thermal conductivity according to geometric average (Equation (12)).

DOI: 10.1002/fam

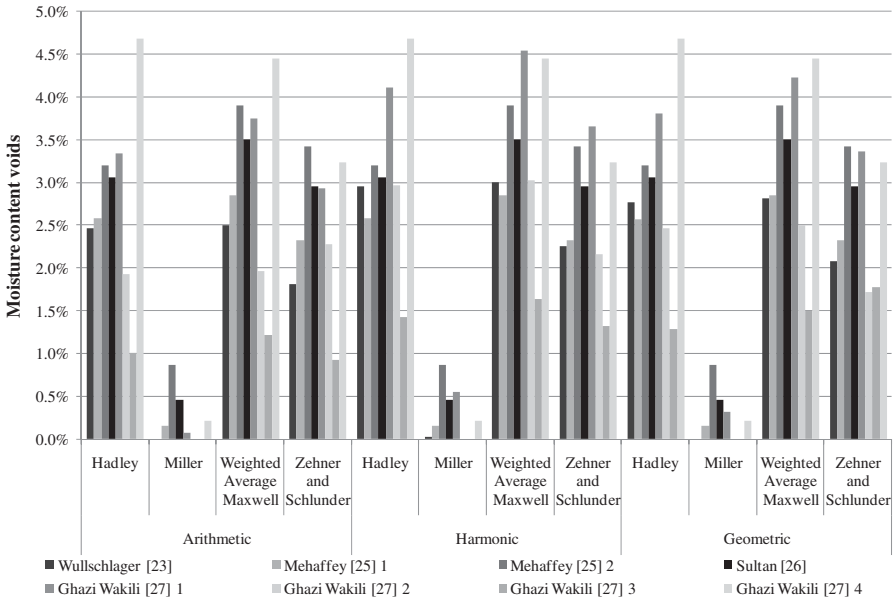

Figure 4. Derived moisture content needed to fit the theoretical and experimental values.

5. APPLICATION TO THERMAL CONDUCTIVITY AT ELEVATED TEMPERATURE

In the previous sections the thermal conductivity at ambient temperatures were analysed. In this section, the developed method is used for the determination of the thermal conductivity during fire, i.e. for elevated temperatures. Therefore, first the reactions during fire are described. The second part will address the comparison between literature and calculations.

5.1. Decomposition reactions

This section will describe the decomposition reactions within gypsum plasterboard during fire. The composition of the plasterboards is described in Section 3. This has an influence on the thermal conductivity, but also will introduce several different decomposition reactions, which are the result of the decomposition of the different substances in the gypsum plasterboard. Calcium sulphate dihydrate will decompose to calcium sulphate hemihydrate at temperatures above 145°C, while hemihydrate will become anhydrite at temperatures above 200°C. Calcium carbonate will react at 800°C to calcium oxide and carbon dioxide.

Based on the presence of these phases, the following reactions can therefore be expected:

$$CaSO_4 \cdot 2H_2O \rightarrow CaSO_4 \cdot \tfrac{1}{2}H_2O + \tfrac{3}{2}H_2O \tag{15}$$

$$CaSO_4 \cdot \tfrac{1}{2}H_2O \rightarrow CaSO_4 + \tfrac{1}{2}H_2O \tag{16}$$

$$CaCO_3 \rightarrow CaO + CO_2 \tag{17}$$

The decomposition reactions are endo-thermal reactions. This is one of the reasons that gypsum plasterboard is used for fire protection since it absorbs the energy of the fire. Table IX summarizes

DOI: 10.1002/fam

Table VIII. Regression analysis of moisture content, in order to investigate its dependence on the chemical composition of the gypsum plasterboards.

		Hypothesis 1			Hypothesis 2			Hypothesis 3			
Equation	Method	M_{solid} (%)	avr (%)	max (%)	M_{gypsum} (%)	avr (%)	max (%)	M_{gypsum} (%)	$M_{carbonate}$ (%)	avr (%)	max (%)
Weighted average Maxwell (Equation (1))	Arithmetic	3.02	0.89	1.80	3.33	0.71	1.76	3.46	−1.71	0.68	1.70
Weighted average Maxwell (Equation (1))	Geometric	3.22	0.81	1.73	3.52	0.67	1.66	3.51	0.11	0.67	1.66
Weighted average Maxwell (Equation (1))	Harmonic	3.37	0.74	1.73	3.65	0.73	1.63	3.52	1.68	0.67	1.69
Hadley (Equation (4))	Arithmetic	2.79	0.79	1.91	3.06	0.63	1.73	3.17	−1.30	0.65	1.69
Hadley (Equation (4))	Geometric	2.98	0.71	1.71	3.25	0.68	1.64	3.21	0.49	0.65	1.65
Hadley (Equation (4))	Harmonic	3.12	0.66	1.70	3.38	0.78	1.61	3.22	2.04	0.66	1.68
Zehner and Schlunder (Equation (9))	Arithmetic	2.48	0.65	1.56	2.62	0.64	1.42	2.80	−2.33	0.57	1.34
Zehner and Schlunder (Equation (9))	Geometric	2.61	0.64	0.89	2.79	0.56	1.32	2.85	−0.80	0.55	1.29
Zehner and Schlunder (Equation (9))	Harmonic	2.67	0.65	1.35	2.91	0.56	1.29	2.86	0.55	0.55	1.30
Miller upper [18]	Arithmetic	0.35	0.29	0.51	0.26	0.22	0.60	0.34	−1.09	0.20	0.52
Miller upper [18]	Geometric	0.40	0.28	0.46	0.29	0.22	0.57	0.36	−0.94	0.20	0.50
Miller upper [18]	Harmonic	0.38	0.28	0.49	0.32	0.25	0.54	0.38	−0.81	0.23	0.47

Avr = average error.
Max = maximum error.

DOI: 10.1002/fam

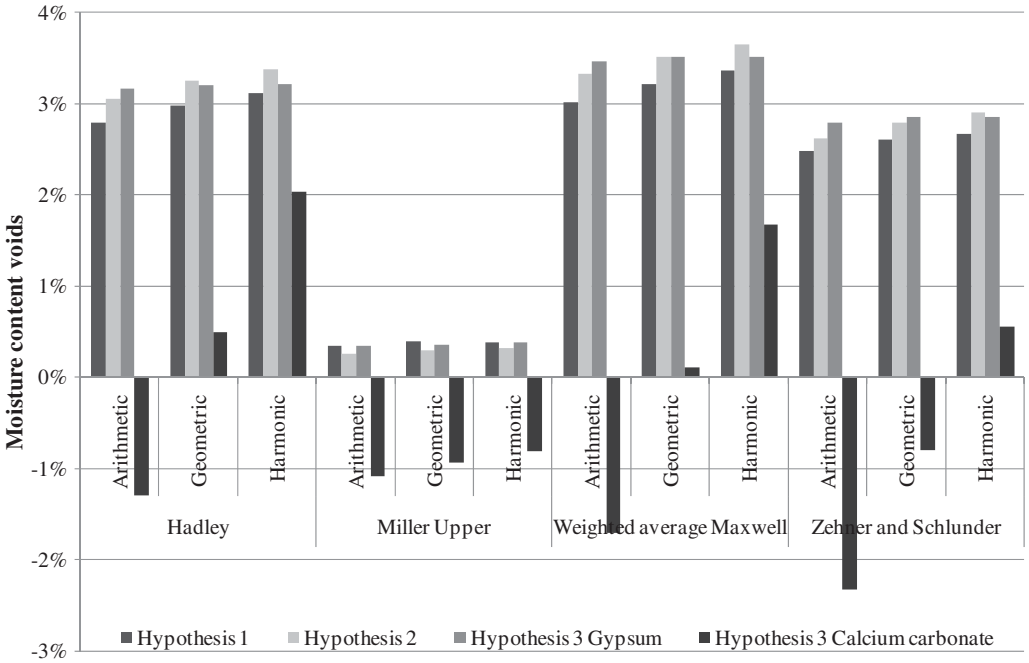

Figure 5. Results for the three hypotheses. Hypothesis 1: moisture content depends on the total mass of the solid. Hypothesis 2: moisture content depends on the mass of the gypsum and hypothesis 3: the moisture content depends on the masses of the gypsum and the limestone.

the reaction temperatures that are needed for the reactions. The previously described reactions are a simplification of decomposition system. Wirsching [34] described the system in more detail.

The dehydration reactions also result in volume changes of the material due to the different specific densities of the phases. Table X shows the volume changes of important reactions within a gypsum plasterboard during heating. The first line of these blocks is the reaction. The second line is the volume of the reaction (in cm^3/mol). The third line gives volume for the reaction of $1\,cm^3$ of dehydration reactant. This line also reveals the volume expansion on percent base. For instance the dehydration of dihydrate leads to shrinkage of the amount of solids with 28.5%, so an increase in void fraction. The assumed reaction temperatures in the model are 145°C for the dehydrate–hemihydrate conversion, 200°C for the hemihydrates–anhydrite conversion and 800°C for the calcium carbonate reaction.

5.2. Model compared with experimental data

The thermal conductivities can now be computed as the composition of the system is known for all temperatures. Figure 6 shows the comparison of the results of the three-phase system with the experimental results of Mehaffey *et al.* [25]. The used properties of the gypsum plasterboard of Mehaffey *et al.* [25] and other important properties are presented in Table XI. Five temperature ranges can be distinguished in Figure 6. At the boundaries of these temperature ranges

DOI: 10.1002/fam

Table IX. Reaction temperatures.

Reaction	Temperature
15	100–120°C [32]
	154°C [33]
16	210°C [32]
	174°C [33]
17	761°C [33]

Table X. Heat needed for and volume changes during dehydration reactions with ΔH_{f0} being the formation heat of substances (kJ/mol), ω being the molar volume (cm^3/mol) and ω_0 being the molar volume of the reactant (cm^3/mol).

	$CaSO_4 \cdot 2H_2O$	$\rightarrow$	$CaSO_4 \cdot \frac{1}{2}H_2O$	+	$\frac{3}{2}H_2O$		Δ
ΔH_{f0}	$-1 \cdot -2022.6$		-1574.6		$\frac{3}{2} \cdot -286$	=	19.0
ω	$-1 \cdot 74.54$		53.33		$\frac{3}{2} \cdot 18$		
ω/ω_0	-1		0.715		0.362	=	0.077
	$CaSO_4 \cdot \frac{1}{2}H_2O$	$\rightarrow$	$CaSO_4$	+	$\frac{1}{2}H_2O$		
ΔH_{f0}	$-1 \cdot -1574.6$		-1424.6		$\frac{1}{2} \cdot -286$	=	7.0
ω	$-1 \cdot 53.33$		53.33		$\frac{1}{2} \cdot 18$		
ω/ω_0	-1		1		0.169	=	0.169
	$CaCO_3$	$\rightarrow$	CaO	+	CO_2		
ΔH_{f0}	$-1 \cdot 1207.0$		-636.0		-393.5	=	450.5
ω	$-1 \cdot 37.07$		16.76		22160		
ω/ω_0	-1		0.452		597.8	=	597.3

the dehydration/decarbonation reactions take place, which will change the chemical composition of gypsum plasterboard. Figure 7 shows these changes in the composition during heating. The thermal conductivity is simulated with the Zehner and Schlunder equation with a shape factor (C) of 5 and an initial moisture content of 2.8% on the gypsum mass is used. This is based on the result from Section 4. The equation of Zehner and Schlunder is used because it depends on few parameters. Furthermore, the thermal conductivities of the solid and fluid phases are assumed to be equal to the data in Table IV, so the thermal conductivities of the individual solid phases are assumed to be constant, i.e. not a function of temperature. Although in reality the thermal conductivity of the composite will slightly change due to changes in density and composition. Also the thermal expansion of the solids is ignored. Upon heating, the solids expand, which reduces the void fraction and the occurrence of complex cracking patterns in case the body is restrained.

Nothwithstanding these and other simplifications, it can be seen from Figure 6 that the simulated value has a good fit with the experimental results from [25]. The raise in thermal conductivity beyond 850°C in the experiments is probably caused by shrinkage cracks in the material. Owin to cracks the air flows through the cracks more easily, and hence increasing the apparent thermal conductivity. This system change is not considered by the present model.

DOI: 10.1002/fam

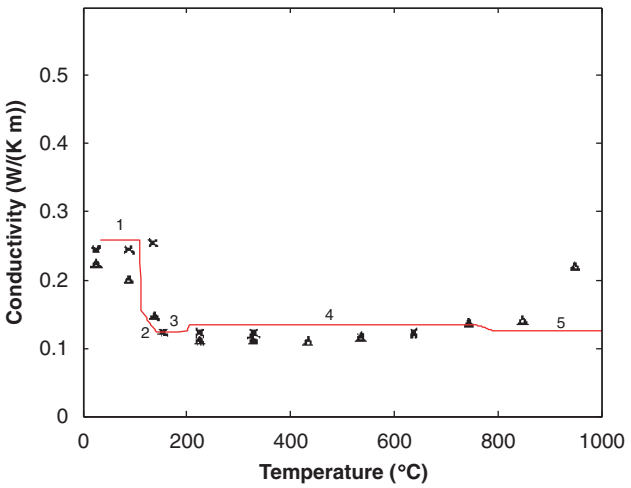

Figure 6. Simulated thermal conductivity according to the proposed model (thin line) and experimental thermal conductivity [25].

Table XI. Starting composition of the plasterboard at 20°C for simulation of the thermal conductivity underlying Figures 6 and 7.

Parameter	Value
Bulk density	732 kg/m^3
Moisture content	3.0% m/m gypsum
Composition	90% gypsum and 10% calcium carbonate
Gypsum	642 kg/m^3
Calcium carbonate	71 kg/m^3
Moisture	19 kg/m^3

6. SUMMARY/CONCLUSION

The thermal conductivity of gypsum plasterboard up to a temperature of 105°C can be described best by a three-phase system as first introduced by Somerton *et al.* [31]. This method requires information about the thermal conductivities that are provided by two-phase systems and the saturation of the voids. The two two-phase systems govern the cases with no saturation and full saturation of the voids.

For the underlying two-phase systems, the Zehner and Schlunder equation with shape factor of 5 yielding good results. Furthermore, a moisture content of 2.8% on the mass of the gypsum should be used in order to adjust the thermal conductivity of the board due to the effect of moisture.

Using this moisture content of 2.8% and the equation of Zehner and Schlunder with $C = 5$ and Somerton, measured values for the thermal conductivity of several plasterboards from literature up to 105°C can be predicted excellently. This amount of moisture content is in line with the values reported in literature, and here it appears to depend only on the gypsum content of the solid phase. For more elevated temperatures, the two-phase equations (air/solid) also proves to be useful, when

DOI: 10.1002/fam

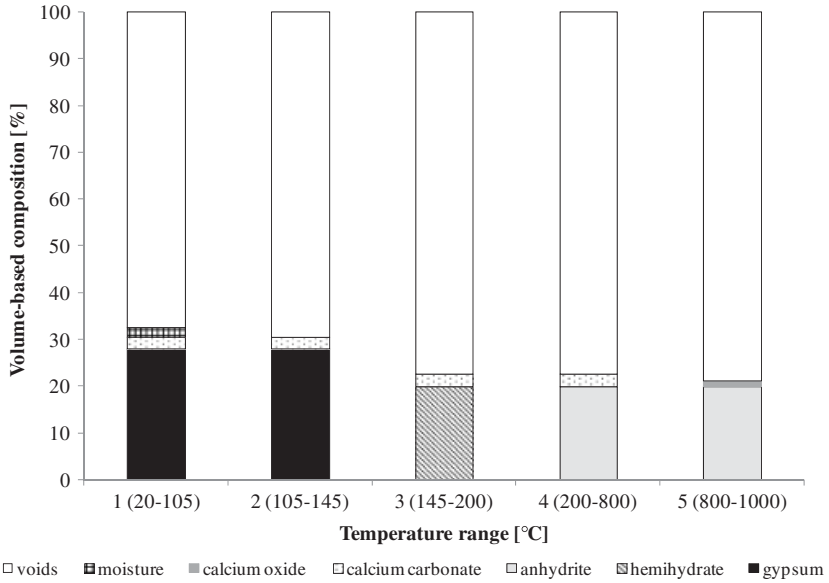

Figure 7. Volumetric chemical composition of the gypsum plasterboard during heating.

one takes the appropriate changes in the type of solid (by dehydration and decarbonation) and related volume (void fraction) changes into account.

APPENDIX: NOMENCLATURE

δ_i	volume fraction of solid phase i
λ_e	effective thermal conductivity of the mix
λ_s	thermal conductivity of the solid
λ_g	effective thermal conductivity of a saturated system with dry air
λ_i	thermal conductivity of the phase i
λ_l	effective thermal conductivity of a saturated system with water
λ_f	thermal conductivity of the fluid in the voids
λ_{meas}	measured thermal conductivity
φ	void fraction
κ	λ_s/λ_f
s_l	saturation rate pore volume water
ρ_e	effective density
ρ	density

ACKNOWLEDGEMENTS

The authors wish to express their sincere thanks to the European Commission (I-SSB Project, Proposal No. 026661-2) and the following sponsors of the research group: Bouwdienst Rijkswaterstaat, Rokramix,

DOI: 10.1002/fam

Betoncentrale Twenthe, Betonmortelcentrale Flevoland, Graniet-Import Benelux, Kijlstra Beton, Struyk Verwo Groep, Hülskens, Insulinde, Dusseldorp Groep, Eerland Recycling, Enci, Provincie Overijssel, Rijkswaterstaat Directie Zeeland, A&G Maasvlakte, BTE, Alvon Bouwsystemen and V.d Bosch Beton (chronological order of joining).

REFERENCES

1. Pignatta e Silva V. Determination of the steel fire protection material thickness by an analytical process—a simple derivation. *Engineering Structures* 2005; **27**(14):2036–2043. DOI: 10.1016/j.engstruct.2005.05.018.
2. Milke J, Kodur V, Marrion C. Overview of fire protection in buildings. World trade center building performance study. *Technical Report*, Federal Emergency Management Agency. Retrieved from http://www.civil.columbia.edu/ce4210/FEMA_403CD/html/pdfs/403_apa.pdf. 2001.
3. Ang C, Wang Y. Effect of moisture transfer on specific heat of gypsum plasterboard at high temperatures. *Construction and Building Materials* 2009; **23**(2):675–686. DOI: 10.1016/j.conbuildmat.2008.02.016.
4. Gawin D, Pesavento F, Schrefler B. Modelling of hygro-thermal behaviour of concrete at high temperature with thermo-chemical and mechanical material degradation. *Computer Methods in Applied Mechanics and Engineering* 2003; **192**(13):1731–1771. DOI: 10.1016/S0045-7825(03)00200-7.
5. Erich SJF, Overbeek ABM, vd Heijden GHA, Pel L, Huinink HP, Peelen WHA, Vervoort A. Validation of FEM models describing moisture transport in heated concrete by magnetic resonance imaging. *HERON* 2008; **53**(4):225.
6. Belmiloudi A, Le Meur G. Mathematical and numerical analysis of dehydratation of gypsum plasterboards exposed to fire. *Applied Mathematics and Computation* 2005; **163**(3):1023. DOI: 10.1016/j.amc.2004.06.013.
7. Takeda H. A model to predict fire resistance of non-load bearing wood-stud walls. *Fire and Materials* 2003; **27**(1):19–39. DOI: 10.1002/fam.816.
8. Manzello SL, Gann RG, Kukuck SR, Lenhert DB. Influence of gypsum board type (X or C) on real fire performance of partition assemblies. *Fire and Materials* 2007; **31**(7):425. DOI: 10.1002/fam.940.
9. Craft ST, Isgor B, Hadjisophocleous G, Mehaffey JR. Predicting the thermal response of gypsum board subjected to a constant heat flux. *Fire and Materials* 2008; **32**(6):333–355. DOI: 10.1002/fam.971.
10. Gerlich JT, Collier PCR, Buchanan AH. Design of light steel-framed walls for fire resistance. *Fire and Materials* 1996; **20**(2):79–96. DOI: 10.1002/(SICI)1099-1018(199603)20:2<79::AID-FAM566>3.0.CO;2-N.
11. Kaviany M. *Principles of Heat Transfer in Porous Media* (2nd edn). Springer: Berlin, 1995.
12. Çengel YA. *Heat and Mass Transfer*: *A Practical Approach*. McGraw-Hill: New York, 2007.
13. Côté J, Konrad JM. Assessment of structure effects on the thermal conductivity of two-phase porous geomaterials. *International Journal of Heat and Mass Transfer* 2009; **52**(1–2):796–804. DOI: 10.1016/j.ijheatmasstransfer.2008.07.037.
14. Hamilton RL, Crosser OK. Thermal conductivity of heterogeneous two-component systems. *Industrial and Engineering Chemistry Fundamentals* 1962; **1**(3):187–191. DOI: 10.1021/i160003a005.
15. Johansen O. Varmeledningsevne av jordarter. *Ph.D. Thesis*, Norge tekniske hogskole, Trondheim, Norway, 1975.
16. Côté J, Konrad JM. A generalized thermal conductivity model for soils and construction materials. *Canadian Geotechnical Journal* 2005; **42**(2):443–458. DOI: 10.1139/t04-106.
17. Maxwell JC. *A Treatise on Electricity and Magnetism*, vol. 1. Clarendon Press: Oxford, 1873.
18. Miller MN. Bounds for effective electrical, thermal, and magnetic properties of heterogeneous materials. *Journal of Mathematical Physics* 1969; **10**(11):1988–2004. DOI: 10.1063/1.1664794.
19. Hadley GR. Thermal conductivity of packed metal powders. *International Journal of Heat and Mass Transfer* 1986; **29**(6):909–920. DOI: 10.1016/0017-9310(86)90186-9.
20. Verma LS, Shrotriya AK, Singh R, Chaudhary DR. Thermal conduction in two-phase materials with spherical and non-spherical inclusions. *Journal of Physics D*: *Applied Physics* 1991; **24**(10):1729–1737. DOI: 10.1088/0022-3727/24/10/006.
21. Zehner P, Schlünder EU. Einfluß der Wärmestrahlung und des Druckes auf den Wärmetransport in nicht durchströmten Schüttungen. *Chemie Ingenieur Technik* 1972; **44**(23):1303–1308.
22. Zehner P, Schlunder EU. Thermal conductivity of granular materials at moderate temperatures. *Chemie Ingenieur Technik* 1970; **42**(14):933–941.
23. Wullschleger L, Ghazi Wakili K. Numerical parameter study of the thermal behaviour of a gypsum plaster board at fire temperatures. *Fire and Materials* 2008; **32**(2):103–119. DOI: 10.1002/fam.956.

24. Ang CN, Wang YC. The effect of water movement on specific heat of gypsum plasterboard in heat transfer analysis under natural fire exposure. *Construction and Building Materials* 2004; **18**(7):505–515. DOI: 10.1016/j.conbuildmat.2004.04.003.
25. Mehaffey JR, Cuerrier P, Carisse G. A model for predicting heat transfer through gypsum-board/wood-stud walls exposed to fire. *Fire and Materials* 1994; **18**(5):297–305. DOI: 10.1002/fam.810180505.
26. Sultan MA. A model for predicting heat transfer through noninsulated unloaded steel-stud gypsum board wall assemblies exposed to fire. *Fire Technology* 1996; **32**(3):239–259.
27. Ghazi Wakili K, Hugi E. Four types of gypsum plaster boards and their thermo-physical properties under fire condition. *Journal of Fire Sciences* 2008; DOI: 10.1177/0734904108094514.
28. Oates T. *Lime and Limestone. Ullmann's Encyclopedia of Industrial Chemistry* Wiley-VCH Verlag GmbH & Co. KGaA: 2008. DOI: 10.1002/14356007.a15_317.
29. Clauser C, Huenges E. Thermal conductivity of rocks and minerals. *Rock Physics and Phase Relations: A Handbook of Physical Constants*, American Geophysical Union, Washington, DC, 1995; 105–126.
30. Bouguerra A. Temperature and moisture dependence on the thermal conductivity of wood-cement-based composite: experimental and theoretical analysis. *Journal of Physics D*: *Applied Physics* 1999; **32**:2797–2803. DOI: 10.1088/0022-3727/32/21/313.
31. Somerton WH, Chu SL, Keese JA. Thermal behavior of unconsolidated oil sands. *Society of Petroleum Engineers of AIME Journal* 1974; **14**(5):513–521.
32. Thomas G. Thermal properties of gypsum plasterboard at high temperatures. *Fire and Materials* 2002; **26**(1): 37–45. DOI: 10.1002/fam.786.
33. Ghazi Wakili K, Hugi E, Wullschleger L, Frank T. Gypsum board in fire—modeling and experimental validation. *Journal of Fire Sciences* 2007; **25**(3):267–282. DOI: 10.1177/0734904107072883.
34. Wirsching F. *Calcium Sulfate. Ullmann's Encyclopedia of Industrial Chemistry*. Wiley-VCH Verlag GmbH & Co. KGaA: Weinheim, 2000. DOI: 10.1002/14356007.a04_555.